

SOFTENING OF PHONON MODES IN  $C_{60}$  CRYSTALS INDUCED BY LASER IRRADIATION: THERMAL EFFECTS

K. P. Meletov<sup>a\*</sup>, E. Liarokapis<sup>b</sup>, J. Arvanitidis<sup>c</sup>,  
K. Papagelis<sup>c</sup>, G. A. Kourouklis<sup>d</sup>, S. Ves<sup>c</sup>

<sup>a</sup> Institute of Solid State Physics, Russian Academy of Sciences  
142432, Chernogolovka, Moscow Region, Russia

<sup>b</sup> Physics Division, National Technical University  
Athens 157 80, Greece

<sup>c</sup> Physics Department, Aristotle University of Thessaloniki  
GR-540 06, Thessaloniki, Greece

<sup>d</sup> School of Technology, Aristotle University of Thessaloniki  
GR-540 06, Thessaloniki, Greece

Submitted 13 March 1998

Reversible softening of the intramolecular  $A_g(2)$  pentagonal pinch (PP) mode of a  $C_{60}$  single crystal in the face centered cubic phase has been studied as a function of laser power density by means of Raman scattering. The average temperature rise in the laser excitation spot has been determined using the Stokes to anti-Stokes integrated peak intensity ratio for the  $H_g(1)$  phonon mode. Softening of the PP-mode was found to be due to heating of the sample resulting from laser irradiation, in good quantitative agreement with experimental results obtained for uniformly heated samples. These findings are in excellent agreement with results obtained by numerical calculations of the local temperature distribution and average temperature in the laser spot based on calculated integrated intensities of the Stokes and anti-Stokes bands of the PP-mode. These calculations were based on experimental data for the temperature dependence of phonon frequency and width, absorbance, and thermal conductivity in solid  $C_{60}$ .

## 1. INTRODUCTION

Raman scattering has been, since the initial discovery of the fullerene family of compounds, a very useful tool for their characterization. In particular, the response of the  $A_g(2)$  PP-mode to a variety of perturbations has been used to probe many diverse properties of solid fullerene and fullerene-based materials. These include temperature- and pressure-induced orientation-ordering phase transitions and effects due to intercalation of solid  $C_{60}$  with alkali metals [1–5]. Raman scattering has also been used to study photodimerization observed in solid  $C_{60}$  under conditions of intense laser illumination, and dimerization caused by high pressure and temperature treatment [6, 7]. The latter effects are clearly manifested by the considerable softening of the  $A_g(2)$  PP-mode.

The frequency of the  $A_g(2)$  mode initially reported by Bethune et al. [8] for the room-temperature Raman spectrum of air-exposed  $C_{60}$  films is  $1469\text{-cm}^{-1}$ . It was also reported that the room-temperature Raman spectrum of oxygen-free  $C_{60}$  contains a broad peak at  $1459\text{ cm}^{-1}$ , which is more intense than the  $1469\text{-cm}^{-1}$  peak. Exposure of the sample to oxygen leads to

\*E-mail: mele@issp.ac.ru

recovery of the  $1469\text{-cm}^{-1}$  peak [9]. The  $1459\text{-cm}^{-1}$  peak in the Raman spectrum of  $C_{60}$  was explained by Rao et al. [6] as a manifestation of the photoassisted dimerization of oxygen-free  $C_{60}$  films under intense laser illumination. It has also been shown that oxygen-exposed  $C_{60}$  films are more resistant to laser irradiation, and need considerably higher laser power densities to initiate the photodimerization reaction [6, 10]. The softening of the PP-mode associated with the photodimerization of  $C_{60}$  is irreversible. The phototransformed material is stable at room temperature and can be recovered only upon heating to temperature greater than 420 K. When the laser illumination level is below the photodimerization threshold, the PP-mode exhibits reversible softening down to  $1461\text{ cm}^{-1}$  [9–11].

Reversible softening of the PP-mode caused by laser illumination has attracted special interest in Raman scattering studies of solid  $C_{60}$ , especially concerning its origin [12]. Raman experiments performed at 40 K have divulged the existence of a second wide band downshifted by  $\sim 3\text{ cm}^{-1}$  from the  $1469\text{-cm}^{-1}$  peak at a laser power density  $\sim 50\text{ W/cm}^2$  [12]. Increasing the laser power density leads to gradual softening and enhancement of the intensity of this band. At the same time, the intensity of the  $1469\text{-cm}^{-1}$  peak goes down, and disappears at a laser power density of  $\sim 300\text{ W/cm}^2$  without any detectable change in peak position. A softening of the new band continues as the power density increases, and becomes irreversible at laser power densities exceeding  $500\text{ W/cm}^2$ . Splitting and softening of the PP-mode is related to the high concentration of molecules in the lowest excited triplet state resulting from the high absorbance of laser radiation, high singlet-triplet intersystem crossing, and the relatively high lifetime of the triplet state [11–13]. It is assumed under these conditions that each intramolecular phonon mode will split into two Raman components that correspond to the PP-mode frequencies in the ground and excited electronic states of the  $C_{60}$  molecule [12].

This assumption, in our opinion, must be examined in light of the photophysics of large molecular systems. It is well established that the frequency of any intramolecular phonon mode of a large molecule, for example an aromatic hydrocarbon, is higher in the electronic ground state than in the excited states [14]. The frequency difference determined via vibrational analysis of the electron-phonon bands in the luminescence and absorption spectra varies from 5 to 10% of the corresponding ground state frequency. Moreover, the frequencies of the corresponding modes in the ground and excited states of a molecule have fixed values and do not depend on the populations of the various states, which are, in turn, related to the laser power density. In  $C_{60}$ , the frequency difference of the split Raman peaks [12] is very small in comparison to the PP-mode frequency, and the change in frequency can be attributed to population of the excited triplet state [12].

From another point of view, laser illumination heats the sample, which, as a rule, is the main reason for phonon mode softening. The heating of solid  $C_{60}$  under laser irradiation, even at low laser power densities, is due to the relatively low thermal conductivity of this material [15]. This has been proposed as an alternative mechanism for PP-mode softening [9, 10].

The experimental study of sample heating due to laser irradiation involves a rather straightforward procedure, and is based on analysis of Raman peak intensities in the Stokes and anti-Stokes regions of the spectrum. We have performed a detailed study of the softening of the PP-mode of solid  $C_{60}$  as a function of the laser power. Our motivation was to examine the relationship between sample heating in the laser spot and PP-mode softening using the relationship between the total intensities of the Stokes  $I_S(\omega)$  to anti-Stokes  $I_{AS}(\omega)$  bands,

$$\frac{I_S(\omega)}{I_{AS}(\omega)} \left[ \frac{\omega_L + \omega}{\omega_L - \omega} \right]^3 = \exp \left( \frac{\hbar\omega}{k_B T} \right), \quad (1)$$

where  $T$  is the mean temperature in the laser spot,  $\omega_L$  is the laser frequency, and  $\omega$  is the phonon frequency, appropriately corrected for the  $\omega^3$  scattering efficiency factor [16]. Effects related to the frequency dependence of the optical coefficients have been neglected, as we are far enough from resonance conditions. We have measured detailed Raman spectra of  $C_{60}$  single crystals in the low-energy Stokes and anti-Stokes regions, as well as in the high-energy region where the PP-mode is located, at room temperature, and at various laser power densities. The results clearly indicate considerable overheating of the sample in the laser spot. They agree well with results on the uniform bath temperature dependence of the PP-mode frequency. We have also performed numerical calculations of the local temperature distribution and the mean temperature in the laser spot from the calculated integrated intensities of the Stokes and anti-Stokes bands of the PP-mode. These calculations were based on experimental data for the absorbance and thermal conductivity of solid  $C_{60}$ , and are in good agreement with the experimental results.

## 2. EXPERIMENTS

Single crystals of fullerite were grown from a solution of  $C_{60}$  in toluene. The primary  $C_{60}$  material, with purity better than 99%, was obtained by the Krätschmer method [17]. Data were recorded on crystals in the form of thin platelets with well-developed specular surfaces and dimensions  $\sim 300 \times 300 \times 50 \mu\text{m}^3$ . The uniform-temperature data were taken using a nitrogen gas flow cryostat, for bath temperatures up to 470 K. In this case the samples were glued to the finger tip using a high-temperature and high thermal conductivity glue. Room-temperature data were taken on freely located air-exposed samples.

Raman spectra were recorded using a triple monochromator (DILOR XY-500) equipped with a CCD cryogenic detector system. The spectral width of the system was  $\sim 5 \text{ cm}^{-1}$ . The 514.5-nm line of an  $\text{Ar}^+$  laser was used for excitation. The laser beam was focused to a spot either  $\sim 1.25 \mu\text{m}$  in diameter using an Olympus 100x objective, or  $\sim 7.5 \mu\text{m}$  in diameter using a Nikon 20x objective with a flux adapter. The laser spot diameter and half-width are critical parameters, along with the laser power, in assessing and comparing experimental results on laser-induced effects. Throughout this paper, we have adopted as the laser spot diameter and half-width the values measured at the 10% and  $1/e$  intensity values relative to the peak, respectively. The spectra were recorded in back-scattering geometry using a  $\lambda/4$  plate as a scrambler and an Olympus microscope system for image processing. The laser power at the sample varied from 0.06 to 0.3 mW for a laser spot diameter  $\simeq 1.25 \mu\text{m}$ , and from 0.4 to 1.5 mW for a laser spot diameter  $\simeq 7.5 \mu\text{m}$ . The data for temperature dependence were recorded at the lowest laser power necessary for recording spectra to minimize the effects of laser irradiation, and the temperature was stabilized for a long time to ensure uniformity over the entire sample volume.

Peak positions and total intensities were determined by fitting Lorentzians to the experimental data. The accuracy of the peak positions was about  $0.25 \text{ cm}^{-1}$ . To eliminate systematic errors in the peak positions, the experimental setup was calibrated before every measurement using the  $17976.7\text{-cm}^{-1}$  plasma line of a Ne lamp, which is located near the PP-mode spectral position. The accuracy of the total peak intensities was limited by the scatter in the background values, and the error was therefore estimated to be no more than 10% of the intensity of the weakest anti-Stokes band. The temperature stabilization accuracy during uniform temperature measurements was  $\sim 1 \text{ K}$ .

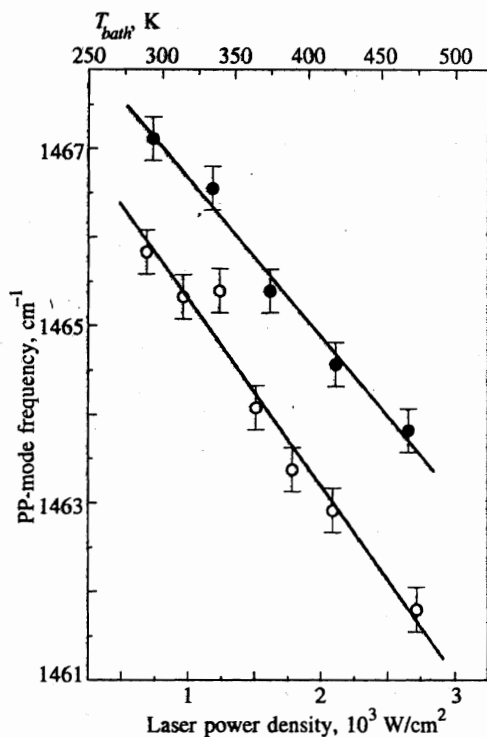


Fig. 1. Dependence of the PP-mode frequency of solid  $\text{C}_{60}$  on laser power density at room temperature, laser spot diameter  $\sim 7.5 \mu\text{m}$  (open symbols). Solid symbols show the dependence of the PP-mode frequency of solid  $\text{C}_{60}$  on the uniform temperature of the sample,  $T_{\text{bath}}$ , for a fixed laser power density  $\sim 200 \text{ W/cm}^2$ . Solid lines are linear least-square fits to the experimental data

### 3. RESULTS AND DISCUSSION

The Raman spectrum of  $\text{C}_{60}$  single crystals, taken at room temperature and normal pressure, contains ten main intramolecular modes:  $H_g(1)$ – $H_g(8)$  and  $A_g(1)$ ,  $A_g(2)$ . Their frequencies are very close to those previously determined: the differences do not exceed  $2\text{--}3 \text{ cm}^{-1}$  [1, 8]. In addition to these bands, there are some very weak Raman peaks that may originate in second-order scattering [18]. The most intense  $A_g(2)$  PP-mode, located under normal conditions at  $\simeq 1467.3 \text{ cm}^{-1}$ , corresponds to the out-of-phase stretching of pentagonal and hexagonal carbon rings.

The frequency of all Raman peaks is sensitive to the laser power density: the majority of the modes soften when the laser power increases. The dependence of the PP-mode frequency on laser power density is shown in Fig. 1 by open symbols. The initial value of the PP-mode frequency  $\simeq 1465.8 \text{ cm}^{-1}$  at laser power density  $\simeq 600 \text{ W/cm}^2$  decreases linearly to  $\simeq 1461.8 \text{ cm}^{-1}$  as the laser power density increases to  $\simeq 2700 \text{ W/cm}^2$ . The extrapolation of this dependence to vanishing laser power density yields a frequency for the PP-mode of  $\simeq 1467.5 \text{ cm}^{-1}$ . This is close to the highest experimental value of  $1467.3 \text{ cm}^{-1}$  observed at minimal laser power density  $\simeq 200 \text{ W/cm}^2$ .

The softening of the PP-mode under laser illumination is reversible when the laser power density increases to  $\simeq 3000 \text{ W/cm}^2$  (for an exposure time of  $\simeq 600 \text{ sec}$ ). At higher laser power densities it becomes irreversible, which case visible damage of the crystal surface at the illumination spot region is observed. The solid symbols in Fig. 1 show the dependence of the PP-mode frequency on the bath temperature,  $T_{\text{bath}}$ , for the uniformly heated samples. The

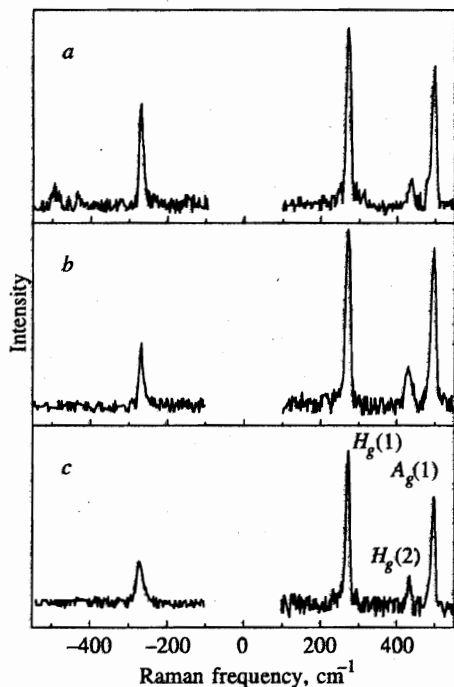


Fig. 2. Raman spectra of solid  $C_{60}$  in the low-energy Stokes and anti-Stokes regions at room temperature, for various laser power levels  $W$ : a) 0.3 mW; b) 0.15 mW; c) 0.06 mW. Laser spot diameter  $\approx 1.25 \mu\text{m}$ ,  $T_{\text{bath}} = 300 \text{ K}$ ,  $T_{\text{spot}}^{\text{exp}}$  is the mean temperature inside the laser spot determined from Eq. (1): a)  $T_{\text{spot}}^{\text{exp}} = 529 \text{ K}$ ; b)  $T_{\text{spot}}^{\text{exp}} = 401 \text{ K}$ ; c)  $T_{\text{spot}}^{\text{exp}} = 340 \text{ K}$

laser power density for this measurements was kept constant at the lowest level,  $\approx 200 \text{ W/cm}^2$ , which corresponds as will be shown, to a local temperature rise of  $\approx 10 \text{ K}$  and a shift in phonon frequency of  $\approx 0.2 \text{ cm}^{-1}$ . These values are close to the experimental accuracy in the peak position and estimated temperature in the laser spot. At room temperature, the frequency of the PP-mode is  $\approx 1467.3 \text{ cm}^{-1}$ , and it decreases to  $1463.7 \text{ cm}^{-1}$  at  $470 \text{ K}$ . The temperature dependence of the PP-mode frequency is very similar to its dependence on laser power density. This is a clear indication that softening of the PP-mode under laser illumination may be related to local overheating of the sample in the laser spot.

Figure 2 shows Raman spectra of the  $C_{60}$  crystal taken in the Stokes and anti-Stokes regions at three different laser power levels. The spectrum in the Stokes region contains three intramolecular phonon modes,  $H_g(1)$ ,  $H_g(2)$ , and  $A_g(1)$ , with frequencies  $273$ ,  $435$ , and  $495 \text{ cm}^{-1}$ , respectively. In the anti-Stokes region, all three spectra contain the prominent  $H_g(1)$  Raman peak. The other two peaks are not detectable at laser powers  $0.06$  and  $0.15 \text{ mW}$ ; they only become visible if the spectrum is recorded at laser power  $\approx 0.3 \text{ mW}$ . The peak intensities of the Raman bands in the Stokes region are essentially the same in all three spectra, whereas in the anti-Stokes region the intensity of  $H_g(1)$  peak increases noticeably as the laser power increases. This is a clear indication that the temperature of the sample within the laser illumination spot gradually increases with laser power.

A comparison of the total intensities of the  $H_g(1)$  Raman peak in the Stokes and anti-Stokes regions on the basis of Eq. (1), using temperature  $T$  as a fitting parameter, yields the average temperature  $T_{\text{spot}}^{\text{exp}}$  in the spot. The data reveal considerable overheating of the sample within the laser illumination spot. The temperature  $T_{\text{spot}}^{\text{exp}}$  reaches  $\approx 530 \text{ K}$  at laser power  $0.3 \text{ mW}$  and spot diameter  $\approx 1.25 \mu\text{m}$ , which is about  $270 \text{ K}$  lower than the heater temperature for the sublimation of  $C_{60}$  powder during vapor growth of fullerite single crystals.

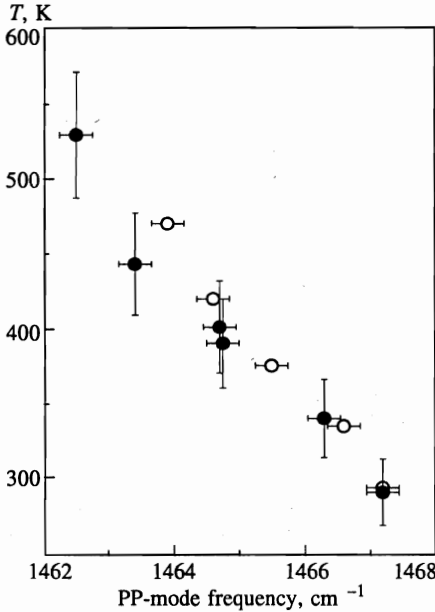


Fig. 3. Dependence of PP-mode frequency of solid C<sub>60</sub> on the uniform temperature of the sample,  $T_{bath}$  (open symbols), and the local temperature inside the laser excitation spot  $T_{spot}^{exp}$  (solid symbols)

These data are compatible with visually observed damage of the crystal surface at high laser powers, when sublimation of material and crater creation takes place due to extreme overheating of the material. As discussed below, the strong temperature rise is due to very low thermal conductivity, which strongly localizes the effect of the laser irradiation.

Figure 3 shows the dependence of PP-mode frequency on the uniform temperature of the sample  $T_{bath}$  (open symbols), and on the mean temperature  $T_{spot}^{exp}$  in the laser spot at various laser powers, determined from Eq. (1) (solid symbols). The agreement between these data is within the experimental errors for the  $T_{spot}^{exp}$  determination, which varies from 20 to 50 K in the various measurements. The results indicate that the temperature of the excited crystal region inside the laser spot,  $T_{spot}^{exp}$ , determined as described above, is significantly higher than room temperature, and increases with laser power. They also mean that the dominant effect of laser illumination is to overheat the sample inside the laser spot, and there is no need to turn to the excited triplet state of C<sub>60</sub> to explain softening of the PP-mode. The relatively high overheating of fullerite with respect to other solids is related primarily to the relatively low thermal conductivity of this material [15].

It can be shown that the resulting laser overheating is compatible with experimental data on light absorbance and thermal conductivity of fullerite [15, 19]. As a check, we have calculated the overheating temperature distribution  $\Delta T(R, Z)$  inside the laser spot from the steady-state solution given originally by Lax [20] for constant thermal conductivity:

$$\Delta T(R, Z) = \frac{I_0 w A (1 - \mathfrak{R})}{K_0} \int_0^\infty d\lambda J_0(\lambda R) F(\lambda) \frac{A e^{-\lambda Z} - \lambda e^{-AZ}}{A^2 - \lambda^2}, \quad (2)$$

where  $\mathfrak{R}$  is the reflectivity,  $K_0$  is the thermal conductivity at room temperature, and  $R = r/w$ ,  $Z = z/w$ ,  $A = \alpha w$  are dimensionless parameters for the radius  $r$ , the depth  $z$ , and the absorption coefficient  $\alpha$ . In the above equation,  $J_0(\lambda R)$  is the zeroth-order Bessel function

and  $F(\lambda)$  is the corresponding Bessel transform of the laser beam profile, which is assumed to be Gaussian, and  $I(r) = I_0 \exp(-r^2/w^2)$ , where  $w$  is the beam half-width at  $1/e$  of the maximum intensity  $I_0$ . In this axial symmetry, the temperature profile depends only on the radius  $r$  and depth  $z$ .

In the above solution, the material is considered semi-infinite, an approximation which is clearly not valid in our case, as the crystallites are of small dimensions. But due to the very low thermal conductivity, the calculations prove that heating is localized, and that it very closely follows the laser beam profile.

The temperature dependence of the thermal conductivity [21] and absorption coefficient [22] has also been considered in the literature. In the present case, the thermal conductivity can be considered constant at  $0.4 \text{ W}\cdot\text{m}^{-1}\cdot\text{K}^{-1}$  above room temperature [15], although more recently even lower values have been reported for the room-temperature thermal conductivity [23]. The optical coefficients can also be considered constant (absorption  $2.7 \mu\text{m}^{-1}$  [19] and reflectivity 0.19 [24]) in the temperature range under consideration. Those two assumptions simplify the calculations considerably. The beam half-width  $w$  was calculated from the value given by the manufacturer of the microscope objective for the excitation wavelength at optimum focusing and for 90% of the total intensity. As all measurements were obtained with the microscope very carefully focused, we can assume that the actual values are very close to optimal, i.e.,  $w = 0.4 \mu\text{m}$  for 100x magnification and  $2.5 \mu\text{m}$  for 20x magnification. In Fig. 4 we present the temperature distribution obtained from Eq. (2) for several laser beam powers and spot diameters  $d = 1.25 \mu\text{m}$  (a) and  $7.5 \mu\text{m}$  (b).

The Raman spectra are given by the convolution of the scattering from volumes ( $2\pi r dr dz$ ) of circular rings of equal temperature at the laser spot. Based on the temperature distribution along the  $r$  and  $z$ -axis obtained from Eq. (2), the Stokes spectra can be calculated from the cross section [16], neglecting the frequency dependence of the second-order susceptibility and the optical constants, as we are far from resonance, i.e.,

$$\frac{dI_s}{d\omega} \propto \int_0^\infty dz \int_0^\infty dr (2\pi r) (1 + \eta) \frac{(\omega_L - \omega)^3}{\omega_{ph}} \frac{\Gamma/2}{(\omega - \omega_{ph})^2 + \Gamma^2/4} I(r) e^{-\alpha z}, \quad (3)$$

where the phonon full FWHM  $\Gamma \approx 5.1 + 0.003(T - 300) \text{ cm}^{-1}$  and the phonon frequency

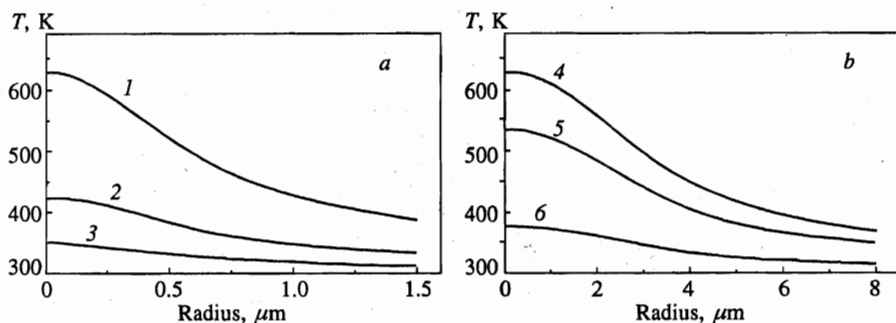


Fig. 4. Temperature distribution as a function of radius inside the laser spot calculated from Eq. (2) and assuming ambient sample temperature  $T_0 = 300 \text{ K}$  and zero depth ( $z = 0$ ). a) Laser spot diameter  $d = 1.25 \mu\text{m}$  and laser power is (1) 0.4; (2) 0.15, and (3) 0.06 mW; b) laser spot diameter  $d = 7.5 \mu\text{m}$  and laser power is (4) 1.6; (5) 1.15, and (6) 0.38 mW

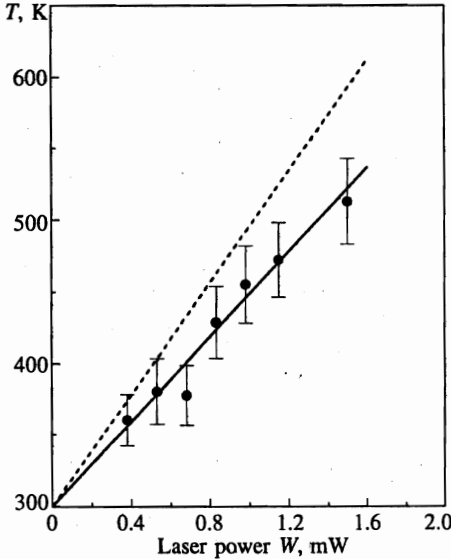


Fig. 5. Temperature in the laser excitation spot as a function of laser power for laser spot diameter  $\approx 7.5 \mu\text{m}$ . Solid symbols are experimental data for  $T_{spot}^{exp}$  determined from the Stokes to anti-Stokes total intensity ratio for the  $H_g(1)$  phonon mode. Solid line is the mean temperature  $T_{spot}^{calc}$ , calculated using Eq. (2) and Eq. (3). Dashed line is the temperature  $T(0, 0)$  at the center of the laser excitation spot and zero depth ( $r = 0, z = 0$ ), calculated using Eq. (2)

$\omega_{ph} \approx 1467 - 0.02(T - 300) \text{ cm}^{-1}$  both depend on the temperature  $T$  in a way defined by the uniform heating (Fig. 1). The statistical factor  $\eta$  is defined in [16]

$$\eta(T) = \frac{1}{\exp(\hbar\omega/k_B T) - 1}. \tag{4}$$

For the anti-Stokes component, the factor  $(1 + \eta)(\omega_L - \omega)^3$  in Eq. (3) must be replaced by  $\eta(\omega_L + \omega)^3$ .

Based on these calculations, the peak position, width, average temperature, and ratio of the Stokes to anti-Stokes total intensities for the  $A_g(2)$  PP-mode can be obtained for every temperature distribution. The calculated average temperature in the spot,  $T_{spot}^{calc}$ , as obtained from the calculated ratio of the Stokes to anti-Stokes total intensities for the PP-mode (corrected for the  $\omega^3$  dependence) are shown in Fig. 5 for  $d = 7.5 \mu\text{m}$ . In the same figure, the data points indicate the experimental results for the average temperature  $T_{spot}^{exp}$  obtained from the ratio of the Stokes to anti-Stokes components of the  $H_g(1)$  phonon mode, also corrected for the  $\omega^3$  dependence. The agreement between the theoretical predictions and the experimental values is remarkable, despite the fact that no adjustable parameters were used in the calculations. This is a strong indication that the modifications induced by laser irradiation in the spectra are due to local heating, which can raise the temperature to 600 K at the center of the laser spot (zero depth), and a power of  $\approx 1.6 \text{ mW}$ , as our calculations indicate for the value of  $T(0, 0)$  (shown by the dashed line in Fig. 5 and calculated from Eq. (2) for  $r = z = 0$ ).

To compare results obtained under various experimental conditions, namely the excitation spot diameter  $d$  and laser power density  $P$ , we found that the results for the average temperature over the spot can be described by the approximate expression

$$\langle T \rangle_{S/AS}^{appr} \approx T_0 + 1116 \frac{W}{d}, \tag{5}$$

where the temperature is given in K,  $T_0$  is ambient temperature, the laser power  $W$  is in mW,

and  $d$  is in  $\mu\text{m}$ . Taking into account that  $W = P\pi d^2/4$ , expression (5) can be written

$$\langle T \rangle_{S/AS}^{pppr} \simeq T_0 + 876Pd. \quad (6)$$

Equation (6) implies that at larger spot diameters, one needs lower laser power densities to achieve the same average temperature rise. This result is consistent with our experimental data obtained for sample overheating at two different spot diameters, and is a very important consideration in trying to compare results obtained under different experimental conditions [6, 8–12]. Equation (6) makes it clear that the power density is not sufficient to compare results on laser-induced overheating of materials with low thermal conductivity.

The calculated temperature profiles inside the laser spot show a considerable difference between the temperature at the center and periphery of the spot. The difference, starting with  $\simeq 30$  K at  $W = 0.2$  mW, reaches  $\simeq 220$  K at  $W = 1.6$  mW (see Fig. 4). The highly nonuniform temperature distribution inside the spot results from the low thermal conductivity of the material. This may be the reason for the splitting of the PP-mode in the Raman spectra taken at temperatures lower than 250 K, the temperature of the orientational-ordering phase transition from fcc to sc structure [25]. According to van Loosdrecht et al. [1], the temperature dependence of the PP-mode frequency exhibits a jump of about  $4\text{ cm}^{-1}$  at 250 K. We remark that in this case the transition temperature of 250 K might be located between the maximum and minimum temperatures within the excitation spot. This means that for a range of laser power densities within the excitation spot, one can have both the low and high temperature phases. The Raman spectra taken under these conditions are expected to show peaks of the PP-mode coming from the two phases, with intensities proportional to the scattering volume corresponding to each phase. At lower and higher laser power densities, the area inside the excitation spot will correspond to a single phase of the material in the low or high temperature phase, respectively. It must be said that this is not exactly the case in Ref. 12, because the laser power densities used are not sufficient to produce the considerable temperature rise within the laser excitation spot. We also think that it might be interesting to extend the measurements of local overheating within the laser spot to the low-temperature region, taking special precautions in the focusing of the laser beam and measuring its power.

#### 4. CONCLUSIONS

Reversible softening of the PP-mode in the Raman spectra of fullerite  $\text{C}_{60}$  under laser illumination is related to overheating of the material inside the laser spot. Estimates of the mean temperature inside the laser spot on the basis of experimental Raman spectra in the Stokes and anti-Stokes regions show that it can reach as high as 530 K at laser power  $\simeq 0.3$  mW and laser spot diameter  $\simeq 1.25\ \mu\text{m}$ . The experimental dependence of PP-mode frequency on the uniform temperature of the sample agrees well with the dependence of the PP-mode position on the mean temperature in the laser spot. Numerical calculations of the local temperature in the laser spot, based on experimental measurements of laser power density, optical absorption, and thermal conductivity of solid  $\text{C}_{60}$ , are in good quantitative agreement with the experimental results.

This work was partially supported by the General Secretariat for Research and Technology, Greece (Grant № 96-1214), the Russian Foundation for Basic Research (Grant № 96-02-17489), the Russian State Program «Fullerenes and Atomic Clusters», and NATO

HTECH. CRG №972317. K. P. Meletov acknowledges the support and hospitality of the Laboratory of Physics, Physics Division, School of Technology, Aristotle University of Thessaloniki, during the course of this work.

## References

1. P. H. M. van Loosdrecht, P. J. M. van Bentum, and G. Meijer, *Phys. Rev. Lett.* **68**, 1176 (1992).
2. N. Chandrabhas, M. N. Shashikala, D. V. S. Muthy, A. K. Sood, and C. N. R. Rao, *Chem. Phys. Lett.* **197**, 319 (1992).
3. K. P. Meletov, D. Christofilos, G. A. Kourouklis, and S. Ves, *Chem. Phys. Lett.* **236**, 265 (1995).
4. Ping Zhou, Kai-An Wang, Ying Wang, P. C. Eklund, M. S. Dresselhaus, G. Dresselhaus, and R. A. Jishi, *Phys. Rev. B* **46**, 2595 (1992).
5. J. Winter and H. Kuzmany, *Sol. St. Commun.* **84**, 935 (1992).
6. A. M. Rao, P. Zhou, K.-A. Wang et al., *Science* **259**, 955 (1993).
7. P.-A. Persson, U. Edlund, P. Jacobsson, D. Johnels, A. Soldatov, and B. Sundqvist, *Chem. Phys. Lett.* **258**, 540 (1996).
8. D. S. Bethune, G. Meijer, W. C. Tang, H. J. Rosen, W. G. Golden, H. Seki, C. A. Brown, and M. S. de Vries, *Chem. Phys. Lett.* **179**, 181 (1991).
9. Y. Hamanaka, S. Nakashima, M. Hangyo, H. Shinohara, and Y. Saito, *Phys. Rev. B* **48**, 8510 (1993).
10. J. Sauvajol, F. Brocard, Z. Hricha, and A. Zahab, *Phys. Rev. B* **52**, 14839 (1995).
11. P. H. M. van Loosdrecht, P. J. M. van Bentum, M. A. Verheijen, and G. Meijer, *Chem. Phys. Lett.* **198**, 587 (1992).
12. P. H. M. van Loosdrecht, P. J. M. van Bentum, and G. Meijer, *Chem. Phys. Lett.* **205**, 191 (1993).
13. Ping Zhou, Zheng-Hong Dong, A. M. Rao, and P. C. Eklund, *Chem. Phys. Lett.* **211**, 337 (1993).
14. V. L. Broude, E. I. Rashba, and E. F. Sheka, *Spectroscopy of Molecular Excitons* [in Russian], Energoizdat, Moscow (1981).
15. R. C. Yu, N. Tea, M. B. Salamon, D. Lorents, and R. Malhotra, *Phys. Rev. Lett.* **68**, 2050 (1992).
16. W. Hayes and R. Loudon, *Scattering of Light by Crystals*, John Wiley & Sons, New York (1978).
17. W. Krätschmer, K. Fostiropoulos, and D. Huffman, *Chem Phys. Lett.* **170**, 167 (1990).
18. Zheng-Hong Dong, Ping Zhou, J. M. Holden, P. C. Eklund, M. S. Dresselhaus, and G. Dresselhaus, *Phys. Rev. B* **48**, 2862 (1993).
19. K. P. Meletov, V. K. Dolganov, O. V. Zharikov, I. W. Kremenskaya, and Yu. A. Ossip'yan, *J. Phys. I France* **2**, 2097 (1992).
20. M. Lax, *J. Appl. Phys.* **48**, 3919 (1977).
21. M. Lax, *Appl. Phys. Lett.* **33**, 786 (1978).
22. E. Liarokapis and Y. S. Raptis, *J. Appl. Phys.* **57**, 5123 (1985).
23. O. Andersson, A. Soldatov, and B. Sundqvist, *Phys. Rev. B* **54**, 3093 (1996).
24. M. Patrini, F. Marabelli, G. Guizzetti, M. Manfredini, C. Castoldi, and P. Milani, in *Recent Advances in the Chemistry and Physics of Fullerenes and Related Materials*, ed. by K. Kadish and R. Ruoff, The Electrochemical Society Inc., Pennington (1994), p. 632.
25. P. A. Heiney, J. E. Fisher, A. R. McGhie, W. J. Romanow, A. M. Denenstein, J. P. McCauley, A. B. Smith, and D. E. Cox, *Phys. Rev. Lett.* **66**, 2911 (1991).